Solubility of uranium oxide in ternary aluminosilicate glass melts

Olivier Podda, Laurent Tissandier, Annabelle Laplace-Ploquin, Etienne Deloule

Solubility of uranium oxide in ternary aluminosilicate glass melts

Olivier Podda[1,2*], Laurent Tissandier[2], Annabelle Laplace[1], Etienne Deloule[2]

[1]CEA, DES, ISEC, DE2D, Laboratoire de Développement des Matrices de Conditionnement, Univ. Montpellier, Marcoule, France
[2]Université de Lorraine, CNRS, CRPG, 54500 Vandoeuvre les Nancy, France

[*]Corresponding Author, E-mail: olivier.podda@hotmail.com

Highlights (should be submitted in a separate file in the online submission)

- Uranium solubility was determined in two simplified glass systems over a wide redox range
- The effect of aluminum content is attributed to the [5]Al proportion
- Uranium volatilization in every MAS system glasses is observed under oxidizing atmospheres

Classification codes (MSC)

86A04 (Geophysics - Experimental work)

Abstract

Uranium solubility was measured in melts belonging to the $CaO-Al_2O_3-SiO_2$ (CAS) and $MgO-Al_2O_3-SiO_2$ (MAS) systems using the Pt wire loop technique, allowing an independent control of the temperature (1400°C), glass composition and the oxygen fugacity ($-16.1 < \log(fO_2) < -0.7$). The low samples mass allowed us to reach the equilibrium state quickly and to perform a rapid quenching of the glasses in order to freeze the system as close as possible to the molten state. The compositions of the different quenched glasses were analyzed by EDS. Uranium solubility decreases with decreasing oxygen fugacity, highlighting the lower solubility of uranium at reduced oxidation states. For each system, uranium solubility is constant from $\log(fO_2) < -9.7$. Moreover, a different uranium behavior is evidenced between the two ternary systems. The modification of Al content affects only uranium solubility in the CAS compositions, while uranium volatilization for oxidizing conditions is noted in the MAS system. These different behaviors may be attributed to structural changes and probably to the variable proportions of [5]Al in each glass system.

KEYWORDS: Uranium, solubility, aluminosilicate glass melt, oxidation states

1. Introduction

The immobilization of highly radioactive waste using vitrification process has been in application since many decades [1] [2] [3]. This process reduces the potential for migration or dispersion of radionuclides [4] by their chemical incorporation into the structure of a glass matrix. This process is now under investigation for conditioning Intermediate Level Waste – Long Life (ILW-LL) - coming from production activities or from decommissioning – and using aluminosilicate glasses as host matrices. These very diverse wastes are highly contaminated with actinides (in particular uranium) and metals can be present. The aim of the process is to solubilize actinides in the molten glass while the decontamination and melting of the metallic parts must be ensured. This involves many additional constraints to the industrial process, such as a potential higher temperature in order to fuse and decontaminate the metallic part, or a wide range of glass compositions and redox conditions. It is therefore essential to get a good understanding of the uranium behavior in glass melts in order to understand the different phenomena operating in nuclear waste immobilization [5] and more generally in U chemistry [6].

The uranium behavior is complex in glass-forming systems due to the presence of various oxidation states. Many studies [7] [8] [9] [10] showed that uranium can be stabilized as U^{VI}, U^{V} and U^{IV} in aluminosilicate, borosilicate and phosphate glasses. To the author's knowledge, only a study has shown that uranium can stabilize into U^{III} at very reduced atmospheres [11]. U^{VI} occurs in the melts as the uranyl ion (UO_2^{2+}) with four to six $U-O_{eq}$ equatorial bonds ($\approx$ 2.21-2.25 Å) and two $U-O_{ax}$ axial bonds ($\approx$ 1.77-1.85 Å) [8] [10] [12]. The planar structure of the uranyl ion could explain the high solubility of U^{VI} in melts. Indeed, when this oxidation state is predominant, uranium solubility in silicate glasses can easily reach 15 mol% UO_2 [7] [11]. U^{V} seems to occur in moderately distorted polyhedral shape with $U^{V}-O \approx 2.19$-2.24 Å [8]. However, this oxidation state is hard to study and data on its solubility are almost inexistent because U^{V} is always detected in equilibrium with U^{VI} and/or U^{IV}. According to Schreiber and al., the solubility of the uranium pentavalent state is closer to U^{VI} than U^{IV} [13], however according to Chevreux and al. U^{V} solubility is near U^{IV} [14]. The uranium tetravalent state occurs in less distorted octahedra with $U^{IV}-O \approx 2.26$-2.29 Å [8]. Contrary to U^{VI}, when U^{IV} is predominant, uranium solubility can hardly reach 5 mol% in silicates [15]. Finally, many parameters can affect uranium solubility and the distribution of uranium oxidation states. Reduced species are favored by high temperature and low oxygen fugacity while the opposites favor oxidized species. The composition effects are difficult to interpret. Changing the composition of a glass causes a change in the glass network, but also affects the values of the redox activity coefficients and the glass basicity. However, increasing the glass basicity seems to favor oxidized species [16]. Mutual interactions between redox couples – for example with cerium – can also perturb the uranium redox equilibrium [17] [18]. It is therefore essential to control all parameters during elaboration of U-doped glasses in order to accurately study uranium incorporation in melts. Only few data about uranium solubility in glasses molten in intermediate and reducing conditions are given in the literature [7] [15] [19]. Moreover, many authors do not specify how they define uranium solubility and experimental conditions are not always explicitly stated, making interpretation of uranium solubility harder.

The main purpose of this paper is to describe the uranium behavior into a glass melt and its evolution as a function of the glass composition and the redox conditions. We present here uranium data in two aluminosilicate systems (CaO-Al_2O_3-SiO_2 and MgO-Al_2O_3-SiO_2) melted under oxygen fugacities ranging from 0.21 (air) to $10^{-16.1}$ atm. Under these conditions, all uranium oxidation states could be investigated while the study of the crystallizations is beyond the scope of this paper.

2. Analytical Procedure

This study aims to analyze uranium solubility in aluminosilicate glass melts. For this purpose, seven U-free compositions (four in the ternary system CaO-Al_2O_3-SiO_2 and three in the ternary system MgO-Al_2O_3-SiO_2) are first synthesized. In each ternary system, there are two endmembers, with different Al_2O_3 contents, and one or two intermediate compositions. These glasses are the host matrices into which uranium is further incorporated. To accelerate the equilibrium within the glass melt and to quench the glass as close as possible to the molten state, small quantities of glass are used (< 50mg). The experiences were performed at nine different oxygen fugacities.

2.1 Synthesis of U-free compositions

Ternary aluminosilicate glass compositions used in this study are given in Table 1. The aluminum content is steadily increased in each glass series while keeping the SiO_2/CaO or SiO_2/MgO ratio constant. Glasses were prepared with the following commercial precursors: SiO_2 (Sifraco, purity ≥ 99.4%); Al_2O_3 (Sigma-Aldrich, purity ≥ 98%); CaO (Sigma-Aldrich, purity ≥ 99.9%); MgO (Prolabo, purity ≥ 96%). After weighting the desired amounts of precursors, the mixtures (≈ 200g for each endmember) were blended in an automatic mixer. C0 and C3 glasses were fused at 1400°C for 3 hours in a platinum crucible (Pt-10%Rh), under air in a muffle furnace. M1 and M3 glasses were fused at 1500°C for 3 hours then equilibrated at 1400°C for 1 hour also in a platinum crucible and under air. Glass melts were quenched to glasses on a stainless steel plate. The amorphous character of the endmembers (C0, C3, M1 and M3) were verified by scanning electron microscopy (Zeiss supra 55, operating at 15kV, using Esprit 2.2 as software) and the homogeneity and composition were assessed by energy dispersive spectroscopy (EDS) with a XFlash 4010 detector and a 15kV accelerating voltage. Glasses were then ground in a planetary mill. Glasses C1, C2 and M2 were obtained by mixing appropriate amounts of the two endmembers compositions and further ground in a planetary mill. To compare C and M series, M1 and M2 glasses are obtained by a molar substitution of CaO by MgO from C2 and C3 glasses respectively.

Glass	C0 (mol%)	C1 (mol%)	C2 (mol%)	C3 (mol%)	M1 (mol%)	M2 (mol%)	M3 (mol%)
SiO_2	57.43 (57.88)	56.28	55.13	53.98 (53.08)	55.13 (54.08)	53.98	52.83 (51.72)
Al_2O_3	6.25 (6.51)	8.13	10.00	11.88 (12.20)	10.00 (10.12)	11.88	13.75 (13.85)
CaO	36.32 (35.61)	35.59	34.87	34.14 (34.72)	0	0	0
MgO	0	0	0	0	34.87 (35.79)	34.14	33.41 (34.43)

Table 1 : Initial nominal glass compositions (mol%). For endmembers, EDS analyses results are shown in brackets.

2.2 Synthesis of U-doped compositions

Uranium being in its most soluble form under oxidizing conditions, doping experiments are performed under atmospheric conditions to ensure a maximum uranium incorporation in the glass melt. Uranium used in this study is a natural one from which all the descendant elements are removed. Uranium is added as U_3O_8 raw materials in the initial glasses amounting to 20wt% UO_2 (~5.5 mol%). The resulting glass and U_3O_8 powders (≈ 500mg) were placed in a platinum crucible (Ø=10mm, h=10mm), in a muffle furnace for 3 hours at 1400°C and glasses were then quenched in air. Pieces of each glass were prepared for SEM and EDS analyses in order to assess the absence of crystallization

(Figure 1) and the homogeneity of the glass matrices (Table 2). All glasses are homogeneous and crystal-free. Sodium contaminations are detected in the UM glass series, likely coming from previous experiments in the same furnace. Remaining glasses were subsequently grounded in a planetary mill.
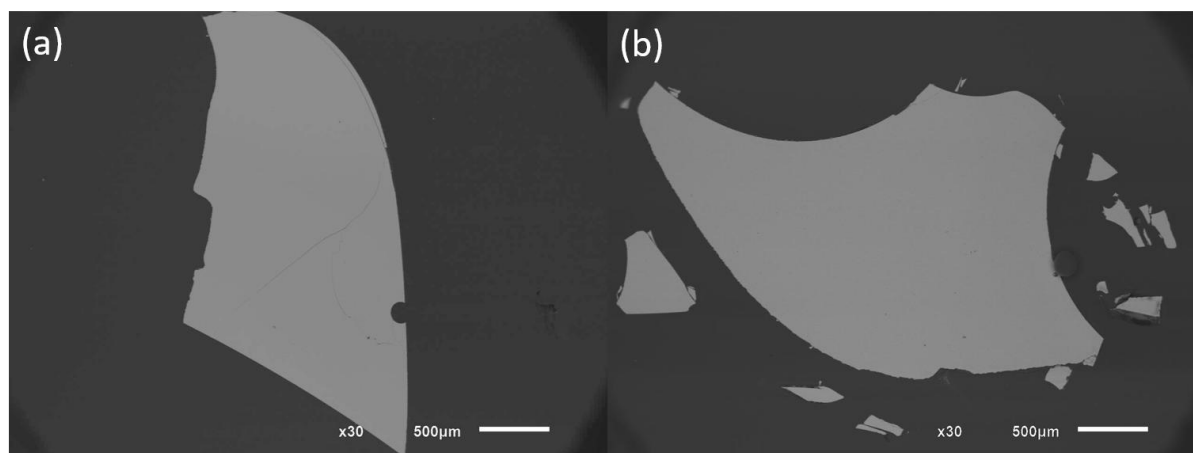

Figure 1. SEM images of (a) UC0 glass and (b) UM3 glass

Glass	UC0 (mol%)	UC1 (mol%)	UC2 (mol%)	UC3 (mol%)	UM1 (mol%)	UM2 (mol%)	UM3 (mol%)
SiO_2	53.69±0.80 (54.35)	53.28±0.55 (53.22)	51.63±0.45 (52.1)	50.71±0.18 (50.98)	51.78±0.46 (52.35)	49.82±0.15 (51.22)	48.59±0.14 (50.09)
Al_2O_3	6.26±0.15 (5.92)	8.42±0.10 (7.69)	10.35±0.09 (9.45)	12.15±0.07 (11.22)	9.80±0.06 (9.50)	11.44±0.08 (11.27)	13.28±0.08 (13.04)
CaO	34.12±0.32 (34.37)	33.14±0.28 (33.66)	32.26±0.23 (32.95)	31.84±0.17 (32.24)	/	/	/
MgO	/	/	/	/	32.81±0.63 (33.11)	33.25±0.16 (32.39)	32.85±0.11 (31.68)
UO_2	5.93±0.77 (5.37)	5.16±0.39 (5.43)	5.75±0.45 (5.50)	5.30±0.10 (5.57)	5.37±0.09 (5.04)	5.29±0.07 (5.12)	5.10±0.11 (5.20)
Na_2O	/	/	/	/	0.23±0.09 (0)	0. 20±0.07 (0)	0.18±0.07 (0)

Table 2: EDS analyses (mol%) of U-doped glasses. Nominal compositions are shown in parentheses. Standard deviation are based on reproducibility of 15 EDS analyses for each glasses.

2.3 Oxygen fugacity imposition

Nine oxygen fugacities have been used in the range $\log(fO_2)$=-0.7 to -16.1 (Table 3). Except for $\log(fO_2)$=-16.1, samples were synthesized using the wire loop technique [20] [21]. Approximately 30 milligrams of uranium-doped glass powder were mixed with polyvinyl alcohol and hung on a platinum wire (or a rhenium wire for $\log(fO_2)$ = 10^{-13} atm). The sample was then attached to an alumina rod and placed in a tubular furnace at 1400°C for 24 hours. The oxygen fugacity was controlled by appropriate calibrated amount of $CO_{(g)}/CO_{2(g)}$ gas mixtures. For $\log(fO_2)$=-16.1, samples were placed in a graphite crucible under a $CO_{(g)}$ atmosphere. After 24 hours, the melt was quenched in air. Due to the low sample mass, the glass matrix quenches in a state equivalent to the molten one.

Log(fO$_2$) (dimensionless, with fO2 (atm))	-3	-4.5	-5.5	-7.5	-9.7	-11	-13	-16.1
Gas mixture (% by volume) %CO$_2$	100	99.1	97.2	78.3	21.7	6.0	0.6	0
%CO	0	0.9	2.8	21.7	78.3	94.0	99.4	100

Table 3 : Oxygen fugacity values imposed by a gas mixture at 1400°C. For log(fo₂)=-16.1, a graphite crucible was used.

2.4 **Uranium solubility measurements**

In this study, uranium solubility refers to the maximum U concentration (expressed as UO$_2$ mol%) in a glass matrix in equilibrium with uranium oxide crystals, i.e. when the saturation of uranium in the melt is reached. Since uranium is added in large quantity, U-oxide crystals should be present in equilibrium with the vitreous phase and confirm that uranium solubility limit is reached.

Quenched glass samples were included in epoxy resin, polished and carbon coated before being characterized. Glass compositions were determined using a Jeol-JSM 6510 scanning electron microscope (SEM) coupled with energy dispersive X-ray spectroscopy (EDS) with a XFlash 5030 detector. The software used is Esprit 2.2. All SEM photos shown in this study were acquired in back-scattered electron mode (BSE). The conditions for EDS analyses were a 15kV acceleration voltage, using virtual controls for the elements quantification. Glass compositions presented here are the average of 30 analyses with 1σ of uncertainties corresponding to the standard deviation for glass samples (15 analyses for checking compositions, Table 2).

3. Results

The aim of this work is to study uranium solubility (by measuring the uranium concentration in the melt, expressed as mol% UO_2) in aluminosilicate glass melts $CaO-Al_2O_3-SiO_2$ and $MgO-Al_2O_3-SiO_2$. Experiments are performed over a wide redox range (from $10^{-0.7}$ atm to 10^{-16} atm) in order to gradually reduce U^{VI} to U^{IV} and determine the U solubility evolution. Several features are developed in this study:

(1) – Validation of the equilibrium state in the samples
(2) – Uranium solubility study in each ternary system
(3) – Impact of the aluminum content in each ternary system
(4) – Comparison of the results for both systems

3.1 Uranium behavior in the melt

In order to study uranium solubility in aluminosilicate glass melts, it is required to control the equilibrium attainment within the melt. Figure 2 shows SEM images of the UC2 glasses for four different redox conditions. None of the glasses synthesized under air (Figure 2a) present uranium crystals. This observation and further EDS analysis allows us to state that uranium solubility limit is not reached for all samples elaborated at fO_2 = 0.21 atm. As expected, as the oxygen fugacity decreases, the amount of crystals increases. Indeed, it seems that less and less uranium can solubilize in the glass melt, and the excess U is incorporated in newly-formed crystals. As in a previous publication [14], two crystal types are observed. The first morphology is isometric and euhedral crystals, whose size is less than 20µm. The second morphology corresponds to dendritic crystals, whose size can easily exceed 100µm. Contrary to UM series, EDS analyses performed on UC glasses, reveal that these crystals are not pure uranium oxide, but may contain calcium impurities.
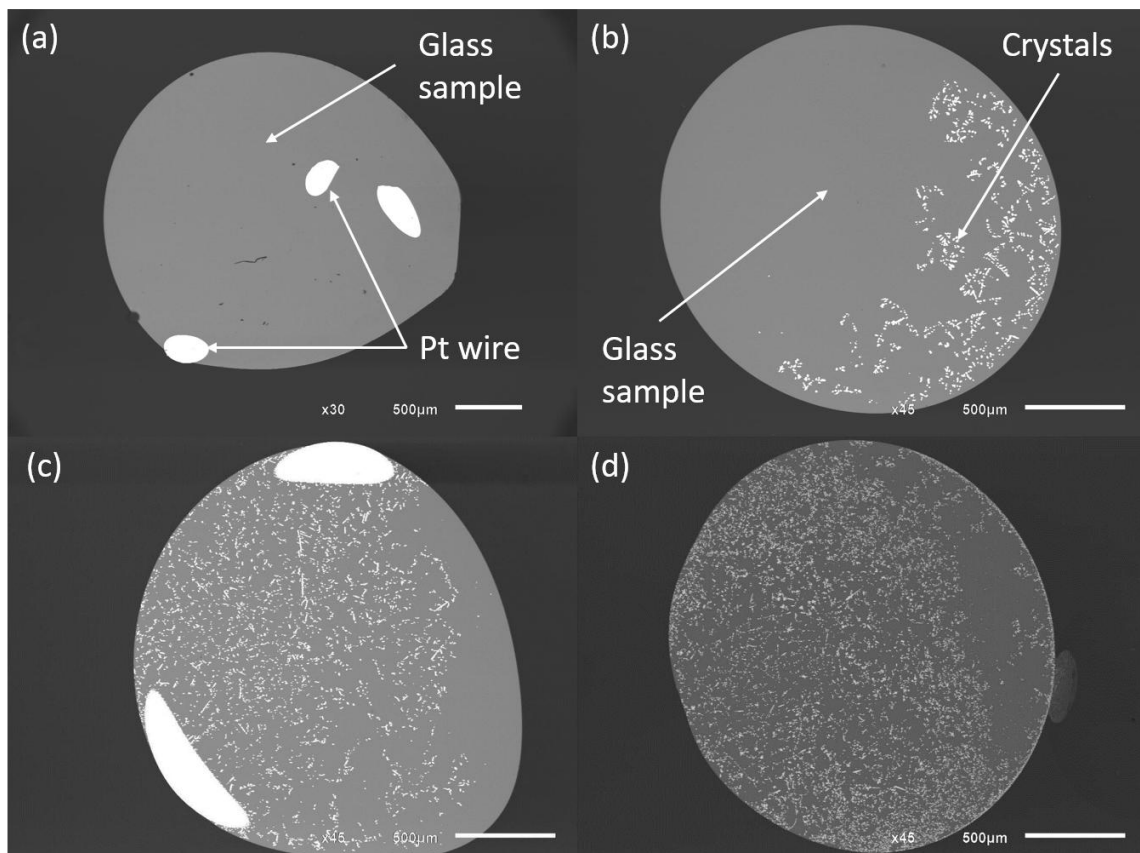
Figure 2. SEM images of UC2 glass samples at (a) log(fO₂) = -0.7 ; (b) log(fO₂) = -3 ; (c) log(fO₂) = -7.5 ; (d) log(fO₂) = -16.1.

Uranium and silicon concentration profiles have been acquired in the crystals vicinity (Figure 3). These profiles show that the uranium content increases abruptly when the amorphous matrix/crystal

boundary is crossed, while in the glass, its concentration remains uniform. This observation leads to the conclusion that the melt is in equilibrium with uranium crystals, and that the crystals were formed by saturation and not during the quenching step. Indeed, even if a crystal overgrowth occurs during this fast cooling, it is very limited because there is no gradient within a few microns from the crystals. Additional evidence proving that the glass melt is in equilibrium with the crystals comes from the absence of a concentration gradient within the matrix as shown by the set of 30 EDS analyses spread over the entire glassy part of the sample (Figure 4). Those observations allow us to conclude that the equilibrium between the melt and the crystals is established in our samples. It should also be noted that some samples were contaminated with Na_2O up to 3 mol% (see Table S1 in supplementary data), certainly coming from the samples synthesis.
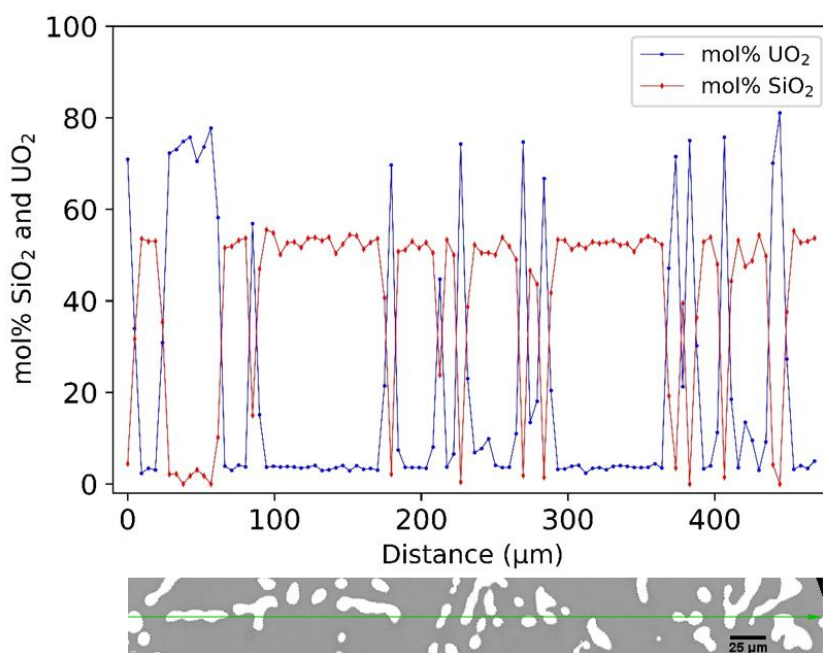
Figure 3. Uranium and silicon concentration profiles
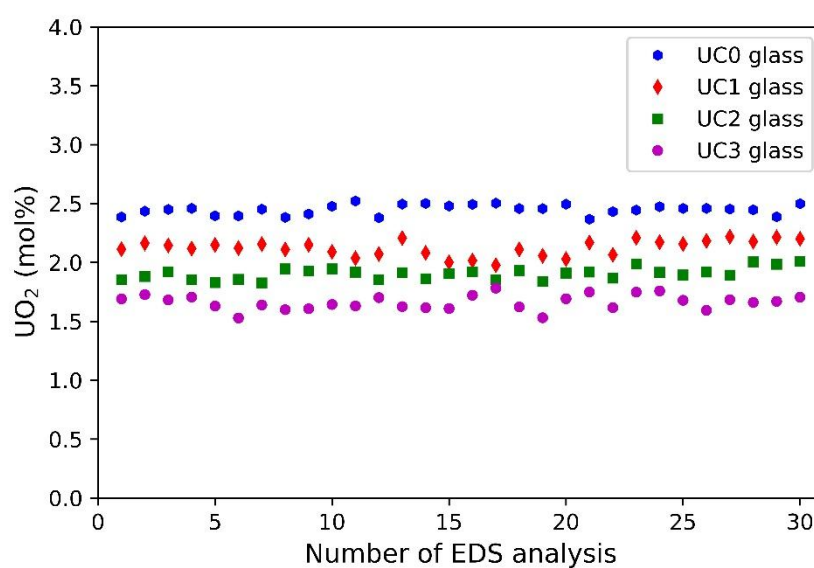
*Figure 4. Total uranium content in mol% UO_2 measured by EDS analyses for each UC glasses synthetized at log(fo₂) = -9.7*

3.2 Uranium solubility

3.2.1 CAS system

The total uranium content in the melt, expressed as UO_2 mol% is plotted as a function of the imposed oxygen fugacity for the different glass compositions in the system $CaO-Al_2O_3-SiO_2$ (Figure 5). All data are available in the Table S1 in supplementary data.

All the compositions follow a similar trend. All the samples elaborated under air ($fO_2=10^{-0.7}$ atm) exhibit a U content around 5.5mol% (~20 wt%, the nominal composition) and no crystals on SEM pictures (Figure 2a) are present. This indicates that uranium solubility is not reached and is higher than 5.5mol% UO_2 under air. For oxygen fugacities going from 10^{-3} atm down to $10^{-9.7}$ atm, uranium solubility progressively decreases while it seems to remain constant in more reducing conditions ($fO_2 < 10^{-9.7}$).

On the other hand, uranium solubility is clearly affected by the aluminum content. For this system, decreasing the aluminum content (from UC3 to UC0 glass) increases uranium solubility, with uranium oxide being about 1.5 times more soluble in UC0 compared to UC3, whatever the fO_2.
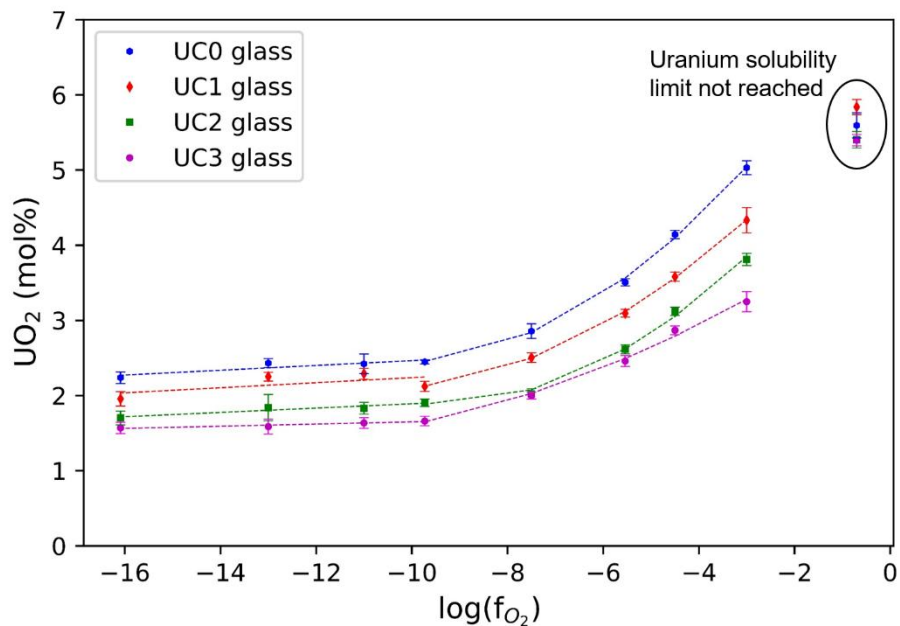
Figure 5. Total uranium content reported as mol% UO_2 as function of oxygen fugacity for UC glasses. Equilibration temperature was 1400°C for 24h. Error bars represent the standard deviation based on reproducibility of 30 EDS analyses for each samples. Dashed lines represent polynomial regressions (degree 2) between $log(fo_2)=-3$ and $log(fo_2)=-9.7$ and simple linear regressions between $log(fo_2)=-9.7$ and $log(fo_2)=-16.1$.

3.2.2 MAS system

As for the CAS system, the total uranium content in the melt is expressed as a function of the imposed oxygen fugacity for different glass compositions in the system $MgO-Al_2O_3-SiO_2$ (Figure 6). From $10^{-4.5}$ atm to $10^{-9.7}$ atm, decrease of uranium solubility (~2.56 mol% to ~1.40 mol%) is similar to CAS system and a plateau is reached at around $fO_2=10^{-9.7}$ atm. Uranium solubility of these glasses is slightly lower than UC3 uranium solubility. Nevertheless, contrary to the former system, changes in the aluminum content in the UM series have no impact on uranium solubility.
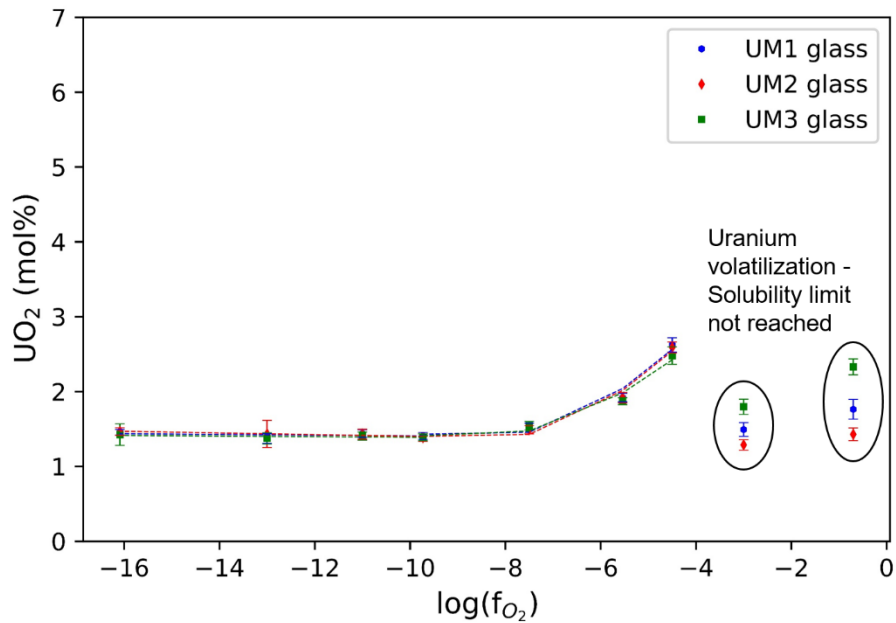
Figure 6. Total uranium content reported as mol% UO_2 as function of oxygen fugacities for each UM glasses. Equilibration temperature was 1400°C for 24h. Error bars represent the standard deviation based on reproducibility of 30 EDS analyses for each samples. Dashed lines represent polynomial regressions (degree 2) between $\log(fo_2)=-4.5$ and $\log(fo_2)=-9.7$ and simple linear regressions between $\log(fo_2)=-9.7$ and $\log(fo_2)=-16.1$.

However, for the two most oxidizing conditions ($fO_2=10^{-0.7}$ atm and $fO_2=10^{-3}$ atm), results do not follow the trend observed on the CAS compositions. Indeed, for these samples, U contents are drastically lower than in the initial doped glasses (Table 2) even though the most soluble U^{VI} should be the dominant oxidation state. Moreover, as no crystals are observed in these 6 glass beads, uranium is probably lost by volatilization. To prove this statement, small samples of glasses from UM series were placed in a vertical furnace at 1400°C under air and for different durations. From the initial U-doped glass compositions (see section 2.2 and Table 2), samples (see Table S2 in supplementary data) show a clear progressive decrease of uranium content without any crystallization (Figure 7). After 40 hours spent in the furnace, only ~10% of the initial U is still present in glass matrices. It can also be noted that uranium content at 24h (Figure 7) are close to those in Figure 6 at $\log(fO_2)=-0.7$, i.e between 1.5 and 2 mol% UO_2.
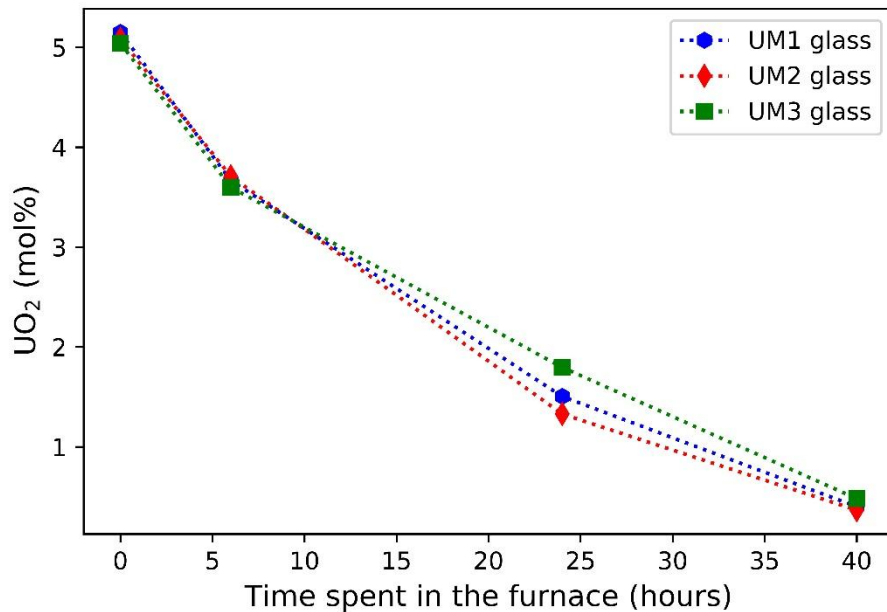
Figure 7. Uranium volatilization in UM glass series under air.

4. Discussion

All the results will now be discussed in the two following paragraphs. The first one deals with uranium solubility in the two different systems (UC and UM glass series) regardless the effect of the composition. The second one discusses the effect of the aluminum content on both uranium solubility and volatilization.

4.1 Uranium solubility

Whatever the composition, uranium solubility decreases while decreasing the oxygen fugacity. For UC glass samples prepared under air, the absence of crystallization on the SEM images (Figure 2a) indicates that uranium solubility limit is not reached. In more reducing environments and whatever the aluminum content for each system, uranium solubility decreases until it reaches a plateau around $10^{-9.7}$ atm (Figure 5 and Figure 6). For lower oxygen fugacities, uranium solubility seems stable. Then, under oxidizing atmosphere, more than 5 mol% UO_2 could be incorporated in the melt at 1400°C whereas in reduced atmosphere, between 1.4 mol% and 2.2 mol% UO_2 are incorporated.

It is well known that the imposed oxygen fugacity modifies the redox equilibria U^{VI}-U^{V}-U^{IV}. At $fO_2 = 0.21$ atm, we postulate a large majority of U^{VI} in the melt leading to a significant solubility (Table 4), which is not reached in our samples. For a lower temperature (1250°C), Chevreux & al. determine that U^{VI} is the sole oxidation state in their samples [14]. However, at 1400°C, there is a possibility that uranium in the U^{V} form is also present. Indeed, in the case of a multivalent element such as uranium, high temperature increases the proportion of reduced species. For a higher processing temperature (1500°C), Schreiber estimates the presence of U^{V} at more than 50% of the total uranium in aluminosilicate melts [13]. When the oxygen fugacity decreases, the U^{VI} oxidation state is progressively reduced to the U^{V} and then to the U^{IV} species. These two oxidation states are less soluble than U^{VI} species. Then, at $fO_2 = 10^{-3}$ and lower, the glass melt becomes supersaturated and uranium oxide crystals precipitate (Figure 2b, c and d) until reaching a crystal/melt equilibrium.

Conditions	Glass type	Sample name	f_{O_2} (atm)	T(°C)	Uranium solubility	Crystallization	Ref
Oxidizing	Aluminosilicates	UC0	air	1400	At least 5.5 mol% UO_2	Absence of crystallization	This study
	Aluminosilicates	UC0-UC3	10^{-3}	1400	Between 5 and 3 mol% UO_2	Presence of crystallization	This study
	Aluminosilicates	AU4	air	1400	At least 4.2 mol% UO_2	Absence of crystallization	[14]
	Borosilicate	U-5	air	1100	At least 4.8 mol% UO_3	Absence of crystallization	[22]
	Aluminosilicates	S-6	air	1250	At least 5.9 mol% UO_2	Absence of crystallization	[23]
	Aluminosilicates	S-7	air	1250	6.8 mol% UO_2	Presence of crystallization	[23]
Intermediate	Aluminosilicate	All samples	$10^{-4.5}$	1400	Between 4.1 and 2.5 mol% UO_2	Presence of crystallization	This study
	Aluminosilicate	All samples	$10^{-5.5}$	1400	Between 3.5 and 1.8 mol% UO_2	Presence of crystallization	This study
	Aluminosilicate	All samples	$10^{-7.5}$	1400	Between 2.9 and 1.5 mol% UO_2	Presence of crystallization	This study
	Aluminosilicate	DI2	$\sim 10^{-7}$	~ 1450	0.7 mol% UO_2	Absence of crystallization	[8]
	Aluminosilicate	AU4-NNO	$10^{-7.1}$	1250	2.3 mol% UO_2	Presence of crystallization	[14]
	Aluminosilicate	AU4-NNO2	$10^{-5.8}$	1400	2.1 mol% UO_2	Presence of crystallization	[14]
	Aluminosilicate	BU4-NNO2	$10^{-5.6}$	1400	2.9 mol% UO_2	Presence of crystallization	[14]
	Potassium aluminosilicate	A 100 K1	10^{-8}	1450	4.18 mol% U_3O_6	Presence of crystallization	[7]
	Potassium aluminosilicate	A 107 B4	10^{-8}	1450	0.06 mol% U_3O_6	Presence of crystallization	[7]
Reducing	Aluminosilicate	All samples	$10^{-9.7}$	1400	Between 2.5 and 1.4 mol% UO_2	Presence of crystallization	This study
	Aluminosilicate	All samples	10^{-11}	1400	Between 2.4 and 1.4 mol% UO_2	Presence of crystallization	This study
	Aluminosilicate	All samples	10^{-13}	1400	Between 2.4 and 1.4 mol% UO_2	Presence of crystallization	This study
	Aluminosilicate	All samples	$10^{-16.1}$	1400	Between 2.4 and 1.4 mol% UO_2	Presence of crystallization	This study
	Aluminosilicate	AU4-IW2	$10^{-9.7}$	1400	1.9 mol% UO_2	Presence of crystallization	[14]
	Aluminosilicate	BU4-IW2	$10^{-9.7}$	1400	1.9 mol% UO_2	Presence of crystallization	[14]

Aluminosilicate	AU4-IW	$10^{-11.3}$	1250	1.2 mol% UO_2	Presence of crystallization	[14]
Aluminosilicate	BU4-C2	10^{-13}	1400	1.7 mol% UO_2	Presence of crystallization	[14]
Aluminosilicate	AU4-C	10^{-15}	1250	1 mol% UO_2	Presence of crystallization	[14]
Aluminosilicate	DI1	~10^{-10}	~1450	0.7 mol% UO_2	Absence of crystallization	[8]

*Table 4. Uranium solubility for different conditions, alongside data reported in the literature for comparison.*

As shown on Figure 5 (between $\log(fO_2)$=-3 and $\log(fO_2)$=-9.7) and Figure 6 (between $\log(fO_2)$=-4.5 and $\log(fO_2)$=-9.7) uranium solubility is at least divided by a factor 2. Within this range, our data do not allow to state which oxidation state is predominant. However, it seems highly probable that this solubility decrease is related to the progressive reduction of U^{VI} (assumed as predominant under air) with decreasing fO_2. For both systems, between $\log(fO_2)$=-9.7 and $\log(fO_2)$=-16.1, the constant solubilities suggests that U^{VI} is not any more present and that i) only U^{IV} is observed or ii) U^{IV} and U^{V} have similar solubilities. However, without XANES analyses, it is not possible to choose between these two hypotheses.

The results of these experiments are in agreement with previous studies. Table 4 compares our results with some other studies for different ranges of redox conditions and similar glass type and elaboration temperatures. It is important to stay careful when comparing data (redox conditions, glass compositions are not always the same, equilibrium attainment…), but our results are in the same range as the previous ones. Under oxidizing conditions, high uranium solubility is found in glasses due to the high solubility of U^{VI}. Moreover and to our knowledge, there is no precise data on uranium crystals under oxidizing conditions (crystals are found in [23] but are not discussed). This may be explained by i) a very high U-solubility in O_2-rich environments, never reached experimentally, or ii) a quick evaporation of U-species preventing the formation of crystals at the solubility limit. Under intermediate and reducing conditions, our data are in the same order of magnitude than results found in the literature.

In order to understand uranium solubility in glass melts, it seems necessary to perfectly know the uranium oxidation states distribution over the redox range. This information is important to know which oxidation state controls uranium solubility, which is still under discussion. Further XAS experiments will be performed on new UC0, UC3 and UM2 samples equilibrated at different fO_2, in order to know the oxidation states distribution and try to predict U^{V} solubility.

4.2 Aluminum effect on the uranium behavior

In both systems, the aluminum content was progressively increased, from 5.92 mol% to 11.22 mol% for UC glasses and from 9.50 mol% to 13.04 mol% for UM glasses (Table 2). This modification in the Al content only affects uranium solubility for the UC glass series (Figure 8). This behavior discrepancy is a demonstration of the different structural roles of Mg and Ca in the silicate melt network and can also be related to the aluminum coordination.
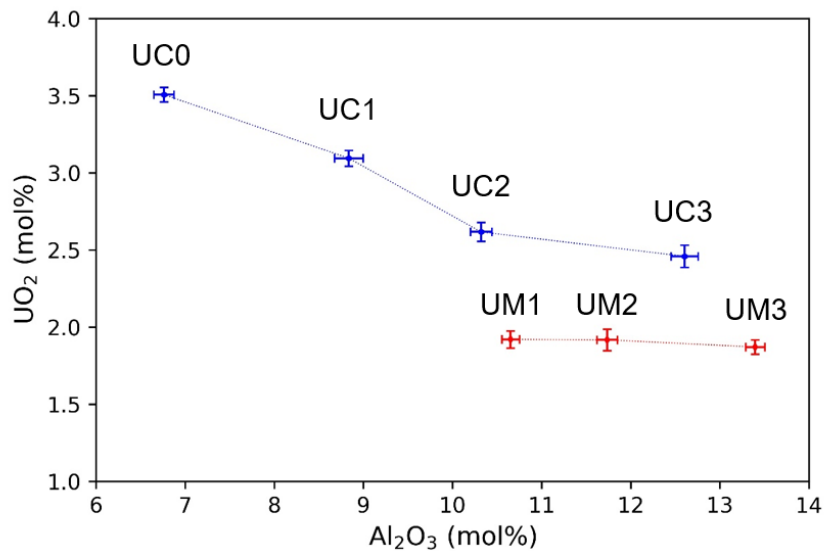
Figure 8. Aluminum effect on uranium solubility for glasses elaborated at log(fo₂)=-5.5. Error bars represent the standard deviation based on reproducibility of 30 EDS analyses for each samples.

Many authors have studied the coordination distribution of aluminum in CAS and MAS glasses. Within a glass network, aluminum is mostly in coordinance 4, this means it forms tetrahedra $(AlO_4)^-$ participating in the network formation but requiring a charge compensator to balance the negative charge. When there is not enough charge compensators within the glass to balance the negative charge of the $(AlO_4)^-$ tetrahedra, the excess aluminum forms high-coordinated Al species, mainly the [5]Al species, some maybe acting as compensators. In the peralkaline region (CaO/Al_2O_3 or MgO/Al_2O_3 > 1, which is the case in our study), even though alkali earth elements can compensate all the Al, authors found that some [5]Al is still present, and in a significantly higher proportion in MAS glasses than in CAS glasses. For example, in reference [24], authors show that the substitution of Ca by Mg increases the [5]Al proportion from 7.6% to 14.3% of the total aluminum content. In addition, the concentration of fivefold coordinated aluminum systematically increases while the ratio CaO/Al_2O_3 decreases at constant silica content [25]. All these observations are in accordance with our data. Figure 9a also shows that increasing the Al/(Al+Si) ratio affects uranium solubility of the UC glass series. For the UC glass series, we can also see that the linear regressions are different as a function of oxygen fugacity.

Under oxidizing conditions, the slopes are steeper and tend to flatten when reaching reducing conditions. However, if we calculate the ratio between uranium solubility of two glasses at the same oxygen fugacity (for example UC0 and UC3), we notice that this ratio remains approximately constant with fO_2 (~1.5). Thus, the composition effects on uranium solubility seem to be the same for each oxygen fugacity. For the UM glass series, the increase in the Al/(Al+Si) ratio does not affect uranium solubility (Figure 9b), allowing the hypothesis of a different effect of Al in these glasses compared to UC series. Changes in the proportions of the uranium oxidation states seem to not affect glass compositions.
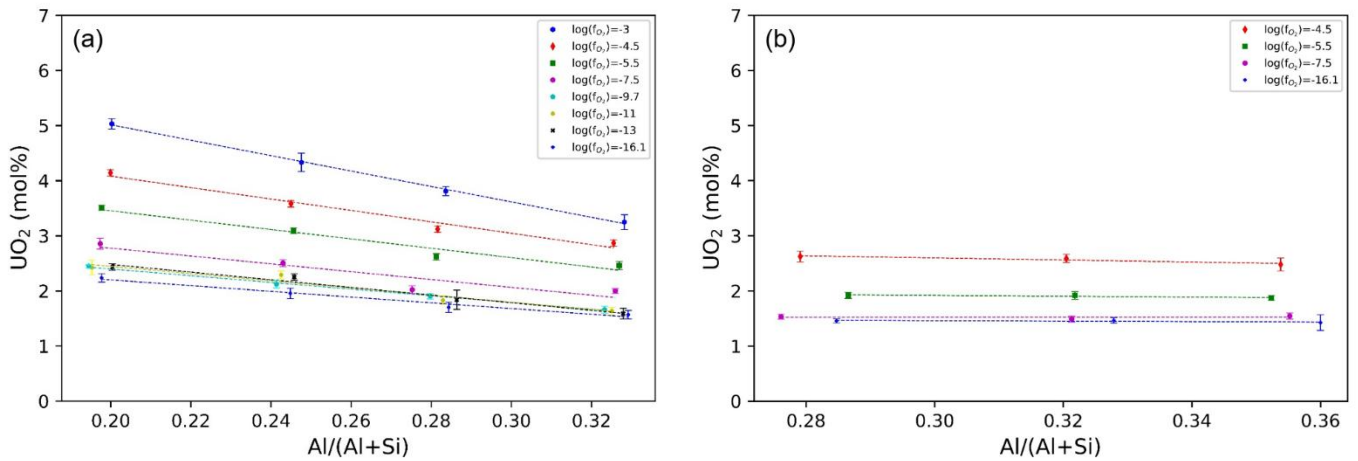
Figure 9. Uranium solubility as a function of Al/(Al+Si) ratio for (a) UC glass system and (b) UM glass system. For UC glasses, low Al/(Al+Si) correspond to UC0 glasses and high Al/(Al+Si) correspond to UC3 glasses. Data for log(fo₂)=-0.7 are not present on this graph because uranium solubility was not reached in these glasses. For UM glasses, low Al/(Al+Si) correspond to UM1 glasses and high Al/(Al+Si) correspond to UM3 glasses. Data for log(fo₂)=-0.7 and log(fo₂)=-3 are not present on this graph because uranium solubility was not reached in these glasses due to uranium volatilization. Data for log(fo₂)=-9.7 to log(fo₂)=-13 are also not represented because they are similar than log(fo₂)=-7.5 and log(fo₂)=-16.1

Uranium volatilization is only detected in the UM glass series and only under oxidizing atmospheres. It is accepted that uranium in its oxidized (i.e. U^{VI}) form is volatile [26] [27] according to the equation:

$$1/3\ U_3O_8 + 1/6\ O_2 = UO_{3(g)} \tag{1}$$

However, this phenomenon appears only in UM glass series meaning that Ca favors the stabilization of U in the silicate melt network compared to Mg. Calcium is found in six (or seven)-fold coordinated ions (and shows a similar modifying role as Na ions) while magnesium ions can be found in five-fold but also in four-fold coordination [28] [29] [30]. This suggests two possible roles for magnesium: Mg can compete with aluminum for network forming positions and will not be available for charge compensations of $(AlO_4)^-$ tetrahedra or Mg is localized in tetrahedral interstices of the network, leading to an important distortion of the aluminosilicate network [30]. It was also noted that Mg perturbs more the aluminosilicate network than Ca [31]. Thus, all these results indicate that the roles of the different elements in the silicate melts are intimately imbricated making it difficult to infer the influence of a particular atom without considering the other ones. Consequently we planned to perform new experiments that will be analyzed through XANES/EXAFS and RMN studies to precise the structure of these different melts. This will bring new insights to the understanding of the processes responsible for U incorporation in the silicate network.

5. Conclusion

To study uranium solubility, two ternary U-doped aluminosilicate systems were used, CAS and MAS with an Al_2O_3 content variation. Each composition was studied over a wide redox range, imposed by a $CO_{(g)}/CO_{2(g)}$ gas mixture. Once equilibrium was reached between the crystals and the melt, a rapid quenching was carried out in order to get an insight of uranium solubility in the glass melt. The data obtained allow us to follow the evolution of uranium solubility by a precise and a wide redox imposition. For atmospheric conditions, uranium solubility limit was not reached. Assuming that the uranium is mostly in the U^{VI} form, the solubility of this valence is greater than 5.5 mol%, whatever the composition. The decrease in oxygen fugacity leads to a reduction in the U^{VI} oxidation state, thus increasing the proportion of U^V and then of U^{IV}. Our results ascertain that these oxidation states are much less soluble than U^{VI}, explaining the decrease in uranium solubility. Around $10^{-9.7}$ atm, uranium solubility stabilizes, allowing us to conclude that U^{IV} becomes the predominant oxidation state and imposes the solubility. Assuming that U^{IV} is the only oxidation state present at log(fO₂)=-16.1

(consistent with data from literature), the solubility of U^{IV} is thus between 2.2mol% and 1.4mol% at 1400°C. For the UC glass series, the increase in the aluminum content decreases uranium solubility while for the UM glass series, no effect is observed. The highest solubility is obtained for calcic glasses with the lower aluminum content. This phenomenon seems to be linked to the different [5]Al proportion in the glass. In order to clarify this, planned NMR-MAS experiments will allow us to quantify the [5]Al proportion in several glasses and verify this hypothesis. For MAS system, we highlight the volatilization phenomenon of uranium attributed to the somewhat different roles of calcium and magnesium in a glass network.

6. Acknowledgments

7. References

[1]   P. Colombo, G. Brusatin, E. Bernardo and G. Scarinci, "Inertization and reuse of waste materials by vitrification and fabrication of glass-based products," *Current Opinion in Solid State and Materials Science, 7(3),* pp. 225-239, 2003.

[2]   J. R. Grover, "High-level waste solidification: why we chose glass," *Radioactive Waste Management, 1(1),* pp. 1-12, 1980.

[3]   I. L. Pegg, I. Joseph and C. H. Oh, Hazardous and radioactive waste treatment technologies handbook, Boca Raton, FL: CRC press, 2001, ch. 4.2.1–27.

[4]   M. I. Ojovan, W. E. Lee and S. N. Kalmykov, An introduction to nuclear waste immobilisation, Elsevier, 2019, ch 1.6.

[5]   H. D. Schreiber, G. B. Balazs, B. J. Williams and S. M. Andrews, "Structural and redox properties of uranium in Ca-Mg-Al-Silicate glasses," *In Scientific basis for nuclear waste management,* vol. 3, 1981.

[6]   H. D. Schreiber, G. B. Balazs and B. J. Williams, "The chemistry of uranium in synthetic silicate liquids," *In Lunar and Planetary Science Conference,* vol. 12, pp. 943-945, 1981.

[7]   F. Dominé and B. D. Velde, "Preliminary investigation of the processes governing the solubility of uranium in silicate melts," *Bulletin de minéralogie, 108(6),* pp. 755-765, 1985.

[8]   F. Farges, C. W. Ponader, G. Calas and G. E. Brown Jr, "Structural environments of incompatible elements in silicate glass/melt systems: II. UIV, UV, and UVI," *Geochimica and Cosmochimica Acta, 56(12),* pp. 4205-4220, 1992.

[9]   K. I. Maslakov, Y. A. Teterin, S. V. Stefanovsky, S. N. Kalmykov, A. Y. Teterin and K. E. Ivanov, "XPS study of uranium-containing sodium-aluminum-iron-phosphate glasses," *Journal of Alloys and Compounds, 712,* pp. 36-43, 2017.

[10] S. V. Stefanovsky, O. I. Stefanovskaya, V. Y. Murzin, A. A. Shiryaev and B. F. Myasoedov, "Oxidation state and coordination environment of uranium in sodium iron aluminophosphate glasses," *In Doklady physical chemistry ,* Vols. 468, No. 1, pp. 76-79, 2016.

[11] H. D. Schreiber and G. B. Balazs, "Chemistry of uranium in borosilicate glasses. Pt. 1. Simple base compositions relevant to the immobilisation of nuclear waste.," *Phys. Chem. Glasses;(United Kingdom), 23(5).,* 1982.

[12] G. S. Knapp, B. W. Veal, D. J. Lam, P. A. P. and H. K. Pan, "EXAFS studies of silicate glasses containing uranium," *Materials Letters, 2(4),* pp. 253-256, 1984.

[13] H. D. Schreiber, "The chemistry of uranium in glass-forming aluminosilicate melts," *Journal of the Less Common Metals, 91(1),* pp. 129-147, 1983.

[14] P. Chevreux, L. Tissandier, A. Laplace, T. Vitova, S. Bahl, F. Le Guyadec and E. Deloule, "Uranium solubility and speciation in reductive soda-lime aluminosilicate glass melts," *Journal of Nuclear Materials, 544,* p. 152666, 2021.

[15] D. J. Lam, B. W. Veal and A. P. Paulikas, "X-ray photoemission spectroscopy (XPS) study of uranium, neptunium and plutonium oxides in silicate-based glasses," 1982.

[16] H. D. Schreiber, B. K. Kochanowski, C. W. Schreiber, A. B. Morgan, M. T. Coolbaugh and T. G. Dunlap, "Compositional dependence of redox equilibria in sodium silicate glasses," *Journal of Non-Crystalline Solids, 177,* pp. 340-346, 1994.

[17] H. D. Schreiber, G. B. Balazs and S. J. Kozak, "Chemistry of uranium in glass- forming melts: Redox interactions of uranium with chromium and iron in aluminosilicates," *Journal of the American Ceramic Society, 66(5),* pp. 340-346, 1983.

[18] H. D. Schreiber, "The chemistry of uranium in glass-forming melts: Redox interactions of U (VI)-U (V)-U (V)-U (IV) with cerium in aluminosilicates," *Journal of Non-Crystalline Solids, 49(1-3),* pp. 189-200, 1982.

[19] Y. I. Matyunin and S. V. Yudintsev, " Immobilization of U3O8 in borosilicate glass in an induction melter with a cold crucible," *Atomic Energy, 84(3),* pp. 173-178, 1998.

[20] C. H. Donaldson, R. J. Williams and G. Lofgren, "A sample holding technique for study of crystal growth in silicate melts," *American Mineralogist: Journal of Earth and Planetary Materials, 60(3-4),* pp. 324-326, 1975.

[21] D. C. Presnall and N. L. Brenner, "A method for studying iron silicate liquids under reducing conditions with negligible iron loss," *Geochimica and Cosmochimica Acta, 38(12),* pp. 1785-1788, 1974.

[22] A. J. Connelly, N. C. Hyatt, K. P. Travis, R. J. Hand, M. C. Stennett, A. S. Gandy and D. C. Apperley, "The effect of uranium oxide additions on the structure of alkali borosilicate glasses.," *Journal of non-crystalline solids, 378,* pp. 282-289, 2013.

[23] C. D. Wirkus and D. R. Wilder, "Uranium bearing glasses in the silicate and phosphate systems.," *Journal of Nuclear Materials, 5(1),* pp. 140-146, 1962.

[24] D. R. Neuville, L. Cormier, V. Montouillout, P. Florian, F. Millot, J. C. Rifflet and D. Massiot, "Structure of Mg-and Mg/Ca aluminosilicate glasses: 27Al NMR and Raman spectroscopy investigations," *American Mineralogist, 93(11-12),* pp. 1721-1731, 2008.

[25] D. R. Neuville, L. Cormier, V. Montouillout and D. Massiot, "Local Al site distribution in aluminosilicate glasses by 27Al MQMAS NMR," *Journal of Non-Crystalline Solids, 353(2),* pp. 180-184, 2007.

[26] R. J. Ackermann and A. T. Chang, "Thermodynamic characterization of the U3O8− zz phase.," *The Journal of Chemical Thermodynamics, 5(6),* pp. 873-890, 1973.

[27] C. A. Alexander, «Volatilization of urania under strongly oxidizing conditions,» *Journal of nuclear materials, 346(2-3),* pp. 312-318, 2005.

[28] A. Pedone, G. Malavasi, M. C. Menziani, U. Segre and A. N. Cormack, "Role of magnesium in soda-lime glasses: insight into structural, transport, and mechanical properties through computer simulations," *The Journal of Physical Chemistry C, 112(29),* pp. 11034-11041, 2008.

[29] D. R. Neuville, L. Cormier, A. M. Flank, V. Briois and D. Massiot, "Al speciation and

Ca environment in calcium aluminosilicate glasses and crystals by Al and Ca K-edge X-ray absorption spectroscopy," *Chemical Geology, 213(1-3),* pp. 153-163, 2004.

[30] M. Guignard and L. Cormier, "Environments of Mg and Al in MgO–Al2O3–SiO2 glasses: A study coupling neutron and X-ray diffraction and Reverse Monte Carlo modeling," *Chemical Geology, 256(3-4),* pp. 111-118, 2008.

[31] A. Navrotsky, G. Peraudeau, P. McMillan and J. P. Coutures, "A thermochemical study of glasses and crystals along the joins silica-calcium aluminate and silica-sodium aluminate," *Geochimica and Cosmochimica Acta, 46(11),* pp. 2039-2047, 1982.

[32] D. R. Neuville, L. Cormier, D. De Ligny, J. Roux, A. M. Flank and P. Lagarde, "Environments around Al, Si, and Ca in aluminate and aluminosilicate melts by X-ray absorption spectroscopy at high temperature," *American Mineralogist, 93(1),* pp. 228-234, 2008.

Supplementary data

	Oxides	UC0 Mol%	σ	UC1 Mol%	σ	UC2 Mol%	σ	UC3 Mol%	σ	UM1 Mol%	σ	UM2 Mol%	σ	UM3 Mol%	σ
Log(fO$_2$) = -0.7	Al$_2$O$_3$	6.04	0.44	8.73	0.13	10.52	0.13	12.40	0.11	10.45	0.08	12.20	0.12	13.85	0.11
	CaO	31.92	1.22	32.38	0.24	32.23	0.34	31.66	0.24	/	/	/	/	/	/
	MgO	/	/	/	/	/	/	/	/	34.99	0.30	34.21	0.24	33.47	0.18
	UO$_2$	5.59	0.17	5.84	0.10	5.40	0.11	5.40	0.08	1.76	0.13	1.43	0.08	2.33	0.11
	Na$_2$O	b.d.l	b.d.l	b.d.l	b.d.l	b.d.l	b.d.l	b.d.l	b.d.l	b.d.l	b.d.l	b.d.l	b.d.l	b.d.l	b.d.l
	SiO$_2$	56.45	1.65	53.05	0.19	51.85	0.19	50.54	0.19	52.79	0.27	52.16	0.27	50.35	0.23
Log(fO$_2$) = -3	Al$_2$O$_3$	6.80	0.07	8.89	0.19	10.43	0.22	12.68	0.16	10.36	0.10	12.23	0.09	13.87	0.13
	CaO	33.56	0.23	32.04	0.42	32.54	0.36	31.50	0.34	/	/	/	/	/	/
	MgO	/	/	/	/	/	/	/	/	35.05	0.17	34.60	0.14	33.62	0.18
	UO$_2$	5.03	0.09	4.33	0.17	3.81	0.08	3.25	0.13	1.49	0.09	1.29	0.07	1.80	0.10
	Na$_2$O	0.30	0.28	0.69	0.20	0.54	0.22	0.68	0.27	0.06	0.25	b.d.l	b.d.l	0.10	0.31
	SiO$_2$	54.31	0.23	54.04	0.34	52.69	0.24	51.89	0.31	53.04	0.27	51.88	0.15	50.60	0.37
Log(fO$_2$) = -4.5	Al$_2$O$_3$	6.82	0.14	8.75	0.16	10.31	0.13	12.47	0.13	9.97	0.07	11.81	0.08	13.44	0.11
	CaO	32.98	0.30	32.23	0.34	32.67	0.27	31.23	0.34	/	/	/	/	/	/
	MgO	/	/	/	/	/	/	/	/	34.04	0.16	33.74	0.18	32.92	0.25
	UO$_2$	4.14	0.06	3.58	0.06	3.12	0.06	2.87	0.06	2.62	0.10	2.59	0.07	2.48	0.12
	Na$_2$O	1.49	0.07	1.51	0.28	1.29	0.10	1.77	0.17	1.88	0.16	1.76	0.27	2.08	0.30
	SiO$_2$	54.57	0.23	53.92	0.22	52.61	0.20	51.66	0.23	51.49	0.21	50.10	0.30	49.09	0.38
Log(fO$_2$) = -5.5	Al$_2$O$_3$	6.76	0.11	8.84	0.16	10.32	0.12	12.60	0.15	10.65	0.10	11.74	0.11	13.40	0.11
	CaO	33.64	0.19	31.93	0.28	32.82	0.37	31.40	0.31	/	/	/	/	/	/
	MgO	/	/	/	/	/	/	/	/	31.23	0.18	33.59	0.30	32.10	0.16
	UO$_2$	3.51	0.05	3.09	0.05	2.62	0.06	2.46	0.07	1.92	0.06	1.92	0.07	1.87	0.05
	Na$_2$O	1.21	0.09	1.86	0.18	1.49	0.12	1.65	0.25	3.16	0.28	3.30	0.30	3.39	0.25
	SiO$_2$	54.88	0.23	54.27	0.19	52.76	0.30	51.90	0.25	53.04	0.34	49.46	0.40	49.24	0.35

Log(fO₂) = -7.5	Al₂O₃	6.81	0.24	8.78	0.18	10.09	0.18	12.61	0.13	10.06	0.08	12.00	0.07	13.75	0.14
	CaO	34.65	0.44	33.50	0.37	34.27	0.45	32.60	0.30	/	/	/	/	/	/
	MgO	/	/	/	/	/	/	/	/	34.14	0.20	34.14	0.18	33.39	0.23
	UO₂	2.86	0.10	2.50	0.06	2.02	0.07	2.00	0.04	1.53	0.04	1.49	0.06	1.55	0.06
	Na₂O	0.28	0.25	0.52	0.26	0.50	0.12	0.62	0.19	1.49	0.22	1.65	0.27	1.40	0.26
	SiO₂	55.40	0.21	54.70	0.24	53.12	0.19	52.17	0.27	52.77	0.27	50.71	0.35	49.92	0.35
Log(fO₂) = -9.7	Al₂O₃	6.78	0.10	8.82	0.16	10.42	0.15	12.62	0.20	10.22	0.10	11.99	0.07	13.70	0.10
	CaO	34.64	0.27	33.51	0.33	33.96	0.34	32.81	0.35	/	/	/	/	/	/
	MgO	/	/	/	/	/	/	/	/	34.58	0.30	34.49	0.27	33.70	0.18
	UO₂	2.45	0.03	2.12	0.07	1.90	0.05	1.66	0.06	1.41	0.05	1.39	0.05	1.39	0.05
	Na₂O	b.d.l	b.d.l	0.10	0.19	0.09	0.19	0.09	0.18	1.05	0.34	1.18	0.20	1.21	0.21
	SiO₂	56.13	0.26	55.44	0.20	53.63	0.28	52.82	0.16	52.73	0.39	50.95	0.34	50.00	0.27
Log(fO₂) = -11	Al₂O₃	6.79	0.11	8.83	0.09	10.68	0.12	12.60	0.12	10.39	0.11	12.19	0.10	13.96	0.10
	CaO	34.87	0.34	33.76	0.24	33.37	0.27	33.45	0.47	/	/	/	/	/	/
	MgO	/	/	/	/	/	/	/	/	35.09	0.17	34.49	0.18	33.73	0.18
	UO₂	2.42	0.13	2.29	0.07	1.83	0.08	1.64	0.07	1.44	0.05	1.43	0.07	1.41	0.05
	Na₂O	b.d.l	b.d.l	b.d.l	b.d.l	b.d.l	b.d.l	b.d.l	b.d.l	b.d.l	b.d.l	0.17	0.39	b.d.l	b.d.l
	SiO₂	55.92	0.28	55.13	0.22	54.12	0.20	52.31	0.43	53.08	0.21	51.72	0.42	50.90	0.18
Log(fO₂) = -13	Al₂O₃	6.98	0.08	8.84	0.16	10.75	0.15	12.75	0.20	10.50	0.12	12.32	0.08	14.00	0.11
	CaO	34.87	0.26	34.67	0.46	33.85	0.56	33.41	0.75	/	/	/	/	/	/
	MgO	/	/	/	/	/	/	/	/	35.16	0.23	34.64	0.18	34.11	0.22
	UO₂	2.43	0.06	2.25	0.06	1.84	0.18	1.59	0.10	1.37	0.07	1.44	0.18	1.37	0.08
	Na₂O	b.d.l	b.d.l	b.d.l	b.d.l	b.d.l	b.d.l	b.d.l	b.d.l	b.d.l	b.d.l	b.d.l	b.d.l	b.d.l	b.d.l
	SiO₂	55.71	0.23	54.24	0.46	53.57	0.50	52.26	0.57	52.97	0.25	51.60	0.26	50.52	0.24
Log(fO₂) = -16	Al₂O₃	6.88	0.12	8.91	0.16	10.63	0.16	12.81	0.26	10.44	0.10	12.43	0.13	14.12	0.15
	CaO	35.04	0.24	34.15	0.33	34.20	0.44	33.41	0.32	/	/	/	/	/	/
	MgO	/	/	/	/	/	/	/	/	35.63	0.28	35.16	0.26	34.26	0.17
	UO₂	2.24	0.08	1.96	0.10	1.70	0.09	1.57	0.07	1.46	0.04	1.47	0.05	1.42	0.14

	Na$_2$O	b.d.l	b.d.l	b.d.l	b.d.l	b.d.l	b.d.l	b.d.l	b.d.l	b.d.l	b.d.l	b.d.l	b.d.l	b.d.l	b.d.l
	SiO$_2$	55.84	0.12	54.99	0.31	53.48	0.31	52.21	0.30	52.47	0.28	50.95	0.34	50.20	0.22

Table S1: Glasses composition (mol%) obtained by averaging 30 EDS analyses performed on the surface of all samples. σ represent the standard deviation (b.d.l means below detection limit).

Glass	Time spent in the furnace (hours)	Oxides (mol%)				
		MgO	Al$_2$O$_3$	SiO$_2$	UO$_2$	Na$_2$O
UM1	0	33.94	9.71	50.93	5.15	0.27
	6	34.90	9.67	50.97	3.67	0.79
	24	36.04	9.77	52.17	1.50	0.51
	40	33.16	10.48	53.13	0.40	2.83
UM2	0	34.22	11.31	48.90	5.08	0.48
	6	34.40	11.31	49.70	3.71	0.88
	24	35.23	11.57	51.18	1.33	0.69
	40	34.13	13.13	49.04	0.37	3.33
UM3	0	33.53	13.04	48.05	5.04	0.35
	6	33.48	12.96	48.93	3.60	1.03
	24	34.02	13.18	50.32	1.80	0.69
	40	35.06	11.48	50.42	0.48	2.57

Table S2: UM glass series composition (mol%) for the volatilization experiments.